

Temperature profiles to characterise groundwater flux in the presence of a fault

Author: Iolanda Campos Haro
Facultat de Física, Universitat de Barcelona, Diagonal 645, 08028 Barcelona, Spain.

Advisor: Pilar Neus Queralt Capdevila, Laura Del Val Alonso
(Dated: June 2021)

Abstract: Vertical steady flow and horizontal flow solutions are presented and analyzed to explain fault-controlled geothermal anomalies. These analyses are applied to data sets from the Eastern Vallès Basin geothermal anomaly, where there is the presence of a fault.

I. INTRODUCTION

Nowadays, the study of heat transport in the subsoil under natural conditions is of great importance due to its implications for the exploration and utilization of the geothermal resources. Fault-controlled geothermal systems are the most frequent geothermal zones in Europe. Therefore, they are good candidates for searching possible applications to the geothermal anomaly present on their surroundings.

It is observed that the geothermal anomaly in this type of systems is produced by the up flowing warm groundwater facilitated by the presence of the fault. The hydraulic characterization of these zones is a key aspect for the development of geothermal reservoirs associated to this field characteristics [1].

There are many methods to approach the study of the fault zone hydrogeology, such as fracture mapping, hydraulic testing, geochemistry analysis, and numerical modelling, among others [2]. The study of heat transport in the fault-controlled area can be used as a tracer for groundwater flow dynamics. One good aspect of using this method is that temperature measurements are easy to perform and the sensors cheap. As temperature distribution depends on the rate and direction of the flowing groundwater, using temperature profiles one can determine the properties of the groundwater flux and have an idea about its distribution beyond the surface.

There is a wide range of publications providing analytical and numerical solutions to estimate thermal properties and flux rates from temperature profiles e.g. [3], [4], [5], [6], although there are few applications in fault-controlled geothermal systems.

The objective of this research is to study two analytical solutions to give an interpretation of several temperature profiles and elucidate the groundwater flow patterns. To do so, I am going to present different optimization models of these solutions, that can be used to explain experimental data obtained on the field and make an hypothesis about the underground permeability distribution and conceptual model. Then, I am going to apply this solutions and its optimizations to experimental data from the Eastern Vallès Basin geothermal anomaly (La Garriga - Samalús, Spain), which is controlled by the presence of a fault. These data sets were obtained by IGME (Instituto Geológico y Minero de España).

II. GOVERNING EQUATIONS

Fourier's Law: Also known as the law of thermal conduction, shows that the heat flux is proportional to the temperature gradient [7]:

$$\dot{q} = -k\nabla T, \quad (1)$$

where \dot{q} is the heat flow (W/m^2), k is the thermal conductivity (W/mK) and ∇T is the temperature's gradient (T in K). Heat conduction occurs in the direction of decreasing temperature. Part of the heat that arrives to the Earth's surface comes from its interior, so temperature increases with depth in the lithosphere. This upward gradient ($30 \text{ }^\circ\text{C/km}$ at shallow levels) can be affected by the groundwater flux.

Advection diffusion equation for heat transport in porous media: This differential expression relates the different mechanisms of heat transport taking place in a porous media with the variation of temperature with time [7]:

$$\frac{\partial T}{\partial t} = \frac{k}{\rho c_p} \nabla^2 T + \frac{A}{\rho c_p} - \vec{v} \cdot \nabla T. \quad (2)$$

The first contribution is the heat conduction term, where ρ is the density of the material (kg/m^3) and c_p is the specific heat at constant pressure (W/mK). This can be expressed as $k/\rho c_p = \kappa$, where κ is the thermal diffusivity (m^2/s), that expresses the ability of the material to lose heat by conduction. The second term is the heat generation, where A is the rate of heat generation (W/m^3). The last one is the advective-transfer term, where \vec{v} is the velocity of the fluid (m/s).

III. VERTICAL STEADY FLOW

A. Bredehoeft and Papadopoulos solution

Bredehoeft and Papadopoulos presented a solution for the advection diffusion equation for heat transport for a case of steady-state vertical flow of groundwater and heat in one dimension without heat generation [3]:

$$\frac{\partial^2 T}{\partial z^2} = \frac{c_0 \rho_0 v_z}{k} \frac{\partial T}{\partial z}, \quad (3)$$

where k is the thermal conductivity of the fluid solid complex, c_0 is the specific heat of the water, ρ_0 its density and v_z the fluid velocity in the z direction, taking downwards as positive.

I have analytically solved the equation to have a better understanding of it. Considering a groundwater flow through a semi-confining layer in which the temperature is measured along its vertical section (Fig.1), allows to determine boundary conditions that the measured temperature profile has to fulfill and solve eq.(3).

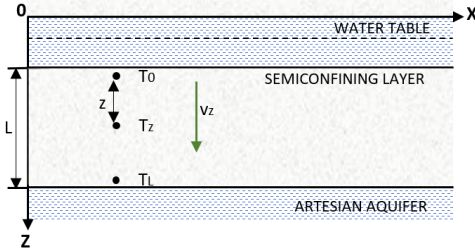


FIG. 1: Sketch of the semi-confining layer model. T_0 is the uppermost temperature measurement, T_L the lowermost temperature measurement, T_z a measured temperature at any point and L is the vertical section where the temperature measurement is made. z -axis positive downwards (modified from [3]).

If the boundary conditions $T_z = T_0$ at $z = 0$ and $T_z = T_L$ at $z = L$ are considered, the solution of eq.(3) is

$$\frac{T_z - T_0}{T_L - T_0} = \frac{e^{\frac{\beta z}{L}} - 1}{e^{\beta} - 1}. \quad (4)$$

β is a dimensionless parameter that is negative if v_z is upwards or positive when downwards. Its expression is $\beta = c_0 \rho_0 v_z L / k$.

Working with this model, having a temperature profile and the properties of the medium, one can determine the vertical groundwater velocity v_z .

B. Sensitivity analysis

I have done a sensitivity analysis for the vertical steady flow solution as shown in Fig.2. I have assumed $T_0 = 0^\circ\text{C}$ and $T_L = 50^\circ\text{C}$ as boundary conditions for both analysis for a layer 160 m deep. For water, $\rho_0 = 1000 \text{ kg/m}^3$ and $c_0 = 4.186 \text{ J/kg}^\circ\text{C}$ [8]. I suppose a semi-confining layer of granite.

On the first analysis, I have represented different values of v_z taking $k = 2,8 \text{ W/m}^\circ\text{C}$ as an average value [8]. The negative value of the velocity indicates upwards groundwater flow. For lower values of velocity, the temperature-depth profile is more linear. High values of temperature are reached near to the surface for increasing values of v_z .

On the second analysis, I have taken different values of k [8]; for $v_z = -0,3 \text{ m/yr}$. As seen in Fig.2b, this model is not very sensitive to variations of k .

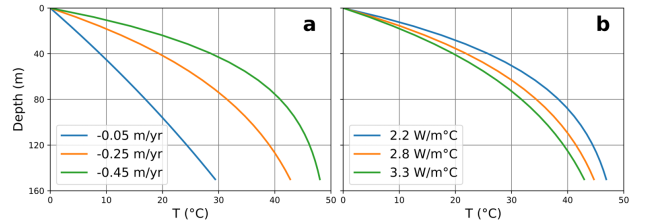


FIG. 2: Sensitivity analysis for the vertical steady flow solution. a) for v_z and b) for k .

C. Application

I have developed two optimization algorithms with Python to adjust the vertical steady flow model to the experimental data. Code can be seen in [9]. In both methods, water and rock parameters are taken as constants. Boundary conditions and the length of the vertical section are obtained from the experimental data set.

In the first method, a theoretical solution is calculated for a given value of v_z with eq.(4). For each v_z , I calculate the mean square error using `sklearn.metrics` [11] between the experimental data and the theoretical solution. When one error value is higher than the previous one, the evaluation stops, taking the previous v_z value as the optimized one. The range of values for v_z has been chosen with the sensitivity analysis.

On the second method, different possible curves for different values of β are calculated. The range of β values has been chosen with the same criteria as in [3]. Then, the main square error between the experimental data and each of the curves is calculated. The β that has the minimum error value is the chosen one. With β one can obtain v_z .

IV. HORIZONTAL FLOW

A. Ziagos and Blackwell solution

Ziagos and Blackwell solution [4] can explain profiles showing temperature inversions. Inversions occur when temperature decreases with depth [6], rather than increase, as it happens at lithosphere if conduction is the only heat transport mechanisms and no heat source is present (e.g. magmatic chamber)[7].

The physical model solved in eq.(2), which explains the inversion temperature profile, is the presence of a discrete confined aquifer buried at depth l containing hot fluid flowing. This thermal water transfers heat to the impermeable rocks above and below. This thin confined aquifer is charged by an upwards flow (Fig.3).

The model is considered time-dependent and two-dimensional (x, z). The thickness of the aquifer is negligible compared with the depth of the layer. No

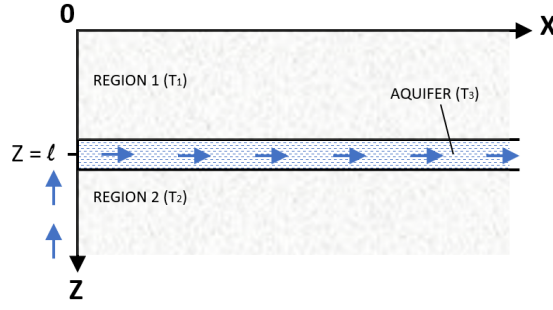


FIG. 3: Sketch of the horizontal flow model. z -axis positive downwards (modified from [4]).

heat generation and no advection in the layers below and above the aquifer is considered. Conduction between aquifer and layers is only on the z direction. With these considerations, eq.(2) becomes

$$\frac{\partial^2 T}{\partial z^2} = \frac{1}{\kappa} \frac{\partial T}{\partial t}. \quad (5)$$

The heat flow in the intersection between the layers and the aquifer along its length, considering no energy generation, is obtained combining eq.(1) and eq.(2):

$$q_1|_{z=l} - q_2|_{z=l} = c_0 \rho_0 a \left[v_f \frac{\partial T_3}{\partial x} + \frac{\partial T_3}{\partial t} \right], \quad (6)$$

where a is the aquifer thickness (m) and v_f is the velocity of the fluid through the aquifer in the x direction (m/yr).

The temperature at any point for initial time and at the surface at any time are set to 0°C . On the charging point ($x = 0$ and $z = l$), the temperature is T_a . For long distances, temperature is supposed to tend asymptotically to 0°C . See *Appendix A* for more details.

I have analytically solved this equations using the Laplace transform method. I have used the long-time approximation assuming that there have not been climatic changes. The solution of the equations is shown in *Appendix A*.

Applying this equations to experimental data, the velocity of the fluid on the x direction, the time since the initiation of the flow, the thermal conductivity of the rock near the aquifer and the temperature of the water at the charger point can be determined.

B. Sensitivity analysis

I have made a sensitivity study to have a feeling about how the equations behave with the different parameters that can be obtained from the horizontal model. Ziagos and Blackwell [4] make an analysis for x variations at constant t and t variations at constant x . I decided to add to the analysis v_f , k and T_a , as they are the target parameters for my application. This sensitivity analysis helped me to decide which parameters may be

the most relevant for the optimization process with the experimental data, and their range of values.

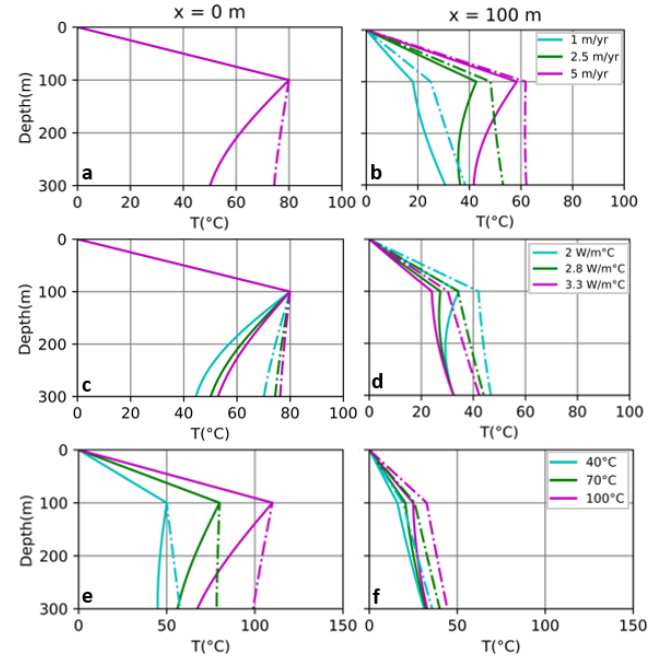


FIG. 4: Sensitivity analysis for the horizontal flow solution. $x = 0$ m in all the plots in the left column, while $x = 100$ m for all plots in the right column. In plots *a* and *b* parameter v_f varies. In plots *c* and *d*, k is the tested parameter. In plots *e* and *f*, T_a is the tested parameter. Continuous lines represent $t = 1000$ yr, while non-continuous line represents $t = 5000$ yr.

The sensitivity analysis is carried out considering x and t constant. I have chosen $x = \{0, 100\}$ m and $t = \{1000, 5000\}$ yr because for higher values there are no important changes. Other constant values are $l = 100$ m, background gradient of $100^\circ\text{C}/\text{km}$, $m_f = 1 \text{ kg/m}^2$, $c_0 = 4,186 \text{ J/kg}^\circ\text{C}$, $\rho = 2000 \text{ kg/m}^3$ and $c_p = 1000 \text{ J/kg}^\circ\text{C}$.

Fig.4 shows some interesting behaviours of this solution. On the upper bedrock layer all profiles are linear except for $v_f = 1 \text{ m/yr}$ and $t = 1000$ yr (Fig.4b). Long-time profiles reach steady-state in both regions for all parameters variations. Finally, the model is not sensitive to variations of v_f and k for $x = 0$ m.

C. Application

To apply this solution to an experimental data set, I have developed an algorithm with Python that fits the theoretical curve with the experimental data. This algorithm is divided in two parts: the preparation of data and the optimization process. Code can be seen in [9].

On the first part of the algorithm, data is standardized to avoid using all the vertical profile but just the part that fits the model. This step is performed because the

presence of the aquifer only affects a specific section of the vertical temperature profile. After this discrimination, the effect of vertical advective transport is subtracted, as it is not considered on the horizontal model. Finally, I normalised the depth of the segment to be analysed, so that it starts at zero. This is done to facilitate the error minimization process.

For the optimization process I used the method `optimize.minimize` from the library `scipy` [10]. This method minimizes a scalar function of one or more variables. The variables are x , t and v_f . I used a constant value for T_a due to the information obtained in the sensitivity analysis. Also, I used $k = 2.65 \text{ W/m}^\circ\text{C}$ [12]. The scalar function to minimize is the calculus of the error between the experimental data and the theoretical profile. The theoretical profile is obtained with eqs.(A7), (A8) and (A9).

The method `optimize.minimize` needs boundary conditions and a range of possible values for each variable. I have chosen the values based on the observations from the sensitivity analysis.

V. FIELD SITE AND TEST DATA

I applied both solutions to different temperature profiles from geothermal anomaly located between La Garriga - Samalús in the the Eastern Vallès Basin (Catalonia, Spain) (Fig.5). In this field site there is a fault with SW direction and $73\text{--}75^\circ$ of inclination. The bedrock is formed by arkose and granite [12]. Some temperature-depth profiles obtained by the IGME on this area show non-linear behavior due to the effect of the geothermal anomaly generated by the fault.

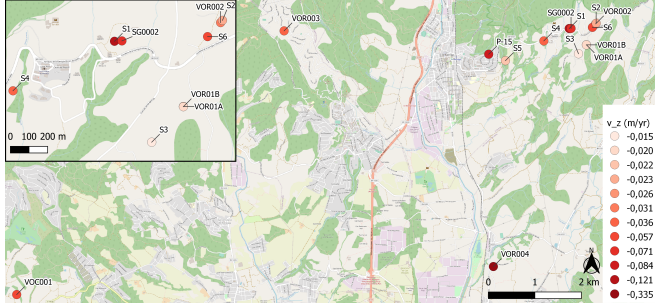


FIG. 5: Map of the field site. Each point is one of the analyzed wells.

VI. RESULTS

A. Vertical steady flow results

I have applied the vertical steady flow solution to fourteen wells from which data is available. With this application, I have obtained the upwards velocity of the groundwater flow taking as constant values $k = 2,65 \text{ W/m}^\circ\text{C}$ (from [12]), $c_0 = 4,186 \text{ J/kg}^\circ\text{C}$ and $\rho_0 = 1000$

kg/m^3 . Adjusted profiles can be seen in *Appendix B* and v_z values in Table I.

Well	v_z (m/yr)	R^2	Well	v_z (m/yr)	R^2
VOR003	-0,036	0,987	S6	-0,057	0,992
P-15	-0,084	0,955	SG0002	-0,071	0,983
S1	-0,121	0,986	VOR01B	-0,020	0,999
S2	-0,023	0,993	VOR002	-0,031	0,989
S3	-0,015	0,998	VOR004	-0,335	0,785
S4	-0,036	0,996	VOC001	-0,057	0,955
S5	-0,022	0,998	VOR01A	-0,026	0,999

TABLE I: v_z for each analyzed well. R^2 is the coefficient of determination.

In Fig.5 one can see that, with the exception of *VOR004*, which is far from the fracture, if the well is near to the fracture close to Samalús, the velocity is higher. *S1* is the well with the highest upwards velocity with $v_z = -0,121 \text{ m/yr}$. The curvature of the profile indicates the importance of the advection contribution in the heat diffusion equation. Taking a look at the adjusted profiles, *S6* is a good candidate to apply the horizontal flow model between $z = 450 \text{ m}$ and $z = 800 \text{ m}$.

B. Horizontal flow results

I have applied the horizontal flow study to the *S6* well between $z = 450 \text{ m}$ and $z = 800 \text{ m}$ (Fig.6). It is important to notice that I used a higher value for the background gradient ($53,5^\circ\text{C/km}$) to adjust the model. The optimization process has determined the values $x = 394,85 \text{ m}$, $t = 8.743 \text{ yr}$ and $v_f = 6.45 \text{ m/yr}$.

VII. DISCUSSION

I have worked with one dimension model for the steady state solution. This allows to make a direct analysis of each term that contributes in the heat transport equation. The study of this equation can be done also with numerical methods. However, numerical methods require a high amount of information which makes analytical methods an ideal tool for an initial interpretation of experimental data and to propose possible conceptual models. Still, these methods are highly idealised and the numerous assumptions need to be considered while applying them.

For the horizontal flow solution I have assumed that for a long time there have not happened changes on the field site. Also, I considered constant values for k and T_a thanks to information from IGME and the sensitivity analysis. If these two parameters are included in the optimization, the result can have a better adjustment.

I have worked without considering the radioactive heat generation of the granite that fills the Vallès basin. With

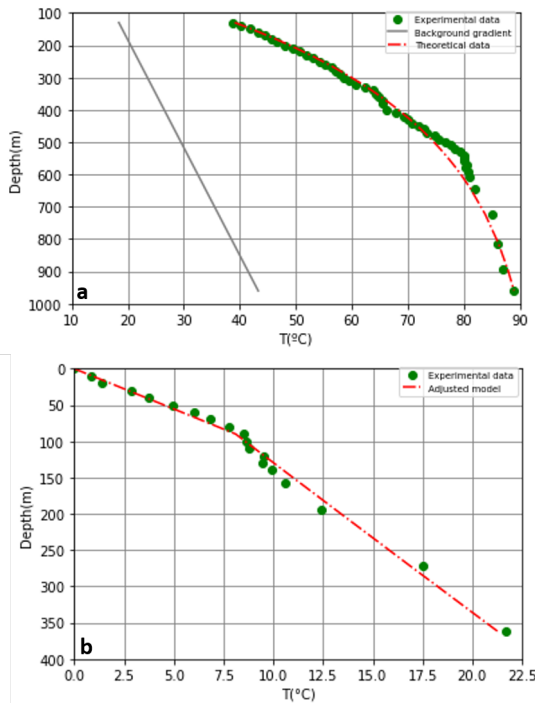


FIG. 6: Result of the optimization process for the S6 well, a) vertical steady flow solution and b) horizontal flow solution.

this consideration, the results could be different.

Although I created two different optimization methods to adjust theoretical and experimental data for the vertical steady flow, I observed that the values obtained for v_z were almost the same except for R^2 . Therefore, I decided to present only the results for the first optimization method, as the obtained R^2 value was closer to 1 in most wells.

With the results of S6, one can see that it is possible to

combine both models to the same data and have an idea about the general circulation of the groundwater flow.

VIII. CONCLUSIONS

- Vertical steady flow solution is not very sensitive to variations of k , so it is a good approximation to use a constant average value if one knows the material present on the studied field.
- The effect of the fault in the groundwater flow is seen with the increasing velocity while we approach to the fracture point.
- Advection effect is shown with the curvature of the profiles. It contributes to increase the velocity.
- The combination of both models allows to determine the circulation on the fault and can be applied to the same experimental data. It allows to make a permeability model of the subsoil.
- As seen in the adjustment of S6 profile, the background gradient of the lithosphere can be altered for the presence of a geothermal anomaly.
- The models studied on this work helps to explain the experimental data obtained in the Eastern Vallès Basin geothermal anomaly (La Garriga - Samalús).

Acknowledgments

I would like to thank Pilar and Laura for their guidance throughout these months to achieve this work. I also want to thank my family, boyfriend and friends for their unconditional support and patience.

-
- [1] Anderson, M. P.. *Heat as a ground water tracer*. Ground Water, 43(6), 951–968, 2005.
[2] Bense, V. F., Gleeson, T., Loveless, S. E., et al. *Fault zone hydrogeology*. Earth-Science Reviews, 127, 171–192, 2013.
[3] Bredehoeft, J. D., Papadopoulos, I. S.. *Rates of Vertical Groundwater Movement Estimated from the Earth's Thermal Profile*. Water Resources Research, 1(2), 1965.
[4] Ziaogos, J. P., Blackwell, D. D.. *A model for the transient temperature effects of horizontal fluid flow in geothermal systems*. Journal of Volcanology and Geothermal Research, 27(3–4), 371–397, 1986.
[5] Sorey, Michael L.. *Measurement of Vertical Groundwater Velocity from Temperature Profiles in Wells*. Water Resources Research, 7(4), 1971.
[6] Bodvarsson, G.. *Temperature inversions in geothermal systems*. Geexploration, 11, 141–149, 1973.
[7] Fowler, C. M. R. *The solid earth: an introduction to global geophysics*. 2nd ed. Cambridge: Cambridge University Press, 2005.
[8] Stauffer, F., Bayer, P., Blum, P., et al. *Thermal use of shallow groundwater*. CRC Press, 2017.
[9] https://github.com/iolan11/tfg_t-profiles
[10] Virtanen, P., Gommers, R., Oliphant, T. E., et al. *SciPy 1.0: Fundamental Algorithms for Scientific Computing in Python*. Nature Methods, 17(3), 261–272, 2020.
[11] Pedregosa, F., Varoquaux G., Gramfort A., et al. *Scikit-learn: Machine Learning in Python*. Journal of Machine Learning Research, 12, 2825–2830, 2011.
[12] IGME, 1977. *Fase preliminar de prospección de recursos geotérmicos de baja entalpía en el Vallés*(Barcelona).
[13] IGME, 1982. *Informe sobre el seguimiento técnico del sondeo SAMALUS-1*.
[14] IGME, 1986. *Proyecto de seguimiento geológico del sondeo de reconocimiento geotérmico SAMALUS-6*.
[15] IGME, 1985. *Proyecto de investigación geotérmica en el Vallés mediante sondeos de reconocimiento y síntesis hidrogeotérmica*.

Appendix A: Horizontal flow equations

Initial condition:

$$T_{1,2,3}(x, z, 0) = 0 \quad (\text{A1})$$

Boundary conditions:

$$T_1(x, 0, t) = 0 \quad (\text{A2}) \quad T_{1,2}(0, l, t) = T_a, \quad t \neq 0 \quad (\text{A3})$$

$$T_{1,2}(x, z, t) \rightarrow 0 \quad \text{as } x \rightarrow \infty, \forall t \neq 0 \quad (\text{A4}) \quad T_2(x, z, t) \rightarrow 0 \quad \text{as } z \rightarrow \infty, \forall t \neq 0 \quad (\text{A5})$$

$$T_1 = T_2 = T_3 \quad \text{at } z = l, \forall x, \forall t \quad (\text{A6})$$

Long-time solution:

$$T_{1(lts)}(x, z, t) = T_a e^{\left(\frac{-\alpha x}{t}\right)} \sum_{n=0}^{\infty} \left[ERFC \left(\frac{(2n+1)l - z + \alpha x}{(4\kappa t'')^{\frac{1}{2}}} \right) - ERFC \left(\frac{(2n+1)l + z + \alpha x}{(4\kappa t'')^{\frac{1}{2}}} \right) \right] \quad (\text{A7})$$

$$T_{2(lts)}(x, z, t) = T_a e^{\left(\frac{-\alpha x}{t}\right)} ERFC \left(\frac{\alpha x + z - l}{(4\kappa t'')^{\frac{1}{2}}} \right) \quad (\text{A8}) \quad T_{3(lts)}(x, l, t) = T_a e^{\left(\frac{-\alpha x}{t}\right)} ERFC \left(\frac{\alpha x}{(4\kappa t'')^{\frac{1}{2}}} \right) \quad (\text{A9})$$

Parameters:

$$\alpha = \frac{k}{m_f c_0 v_f} \quad (\text{A10}) \quad t'' = t - \frac{x}{v_f} - \frac{\alpha x}{3\kappa} \quad (\text{A11})$$

m_f = mass per area of the fluid in the aquifer

k = thermal conductivity of the rock

Appendix B: Vertical steady flow adjusted profiles

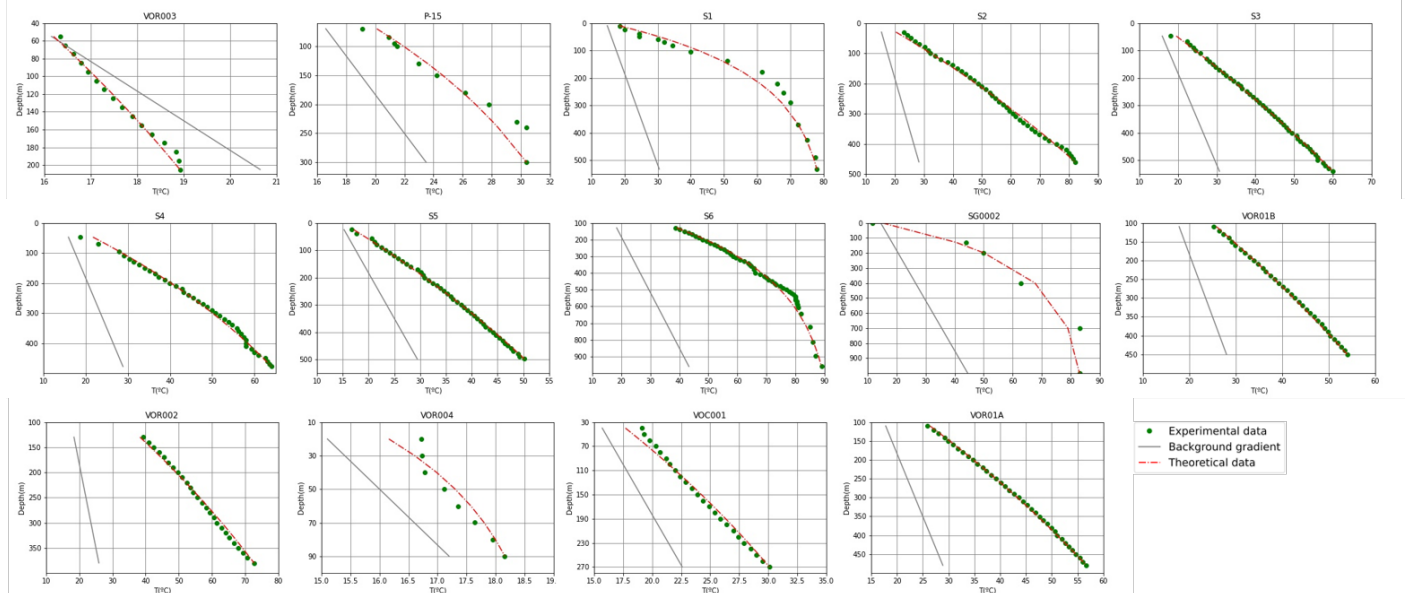


FIG. 7: Adjusted profiles with the vertical steady flow solution for wells from the Eastern Vallès Basin geothermal anomaly (La Garriga - Samalús, Spain).